Effect of pressure on the neutron spin resonance in the unconventional superconductor FeTe_{0.6}Se_{0.4}

K. Marty, A. D. Christianson, A. M. dos Santos, B. Sipos, K. Matsubayashi, Y. Uwatoko, J. A. Fernandez-Baca, C. A. Tulk, T. A. Maier, B. C. Sales, and M. D. Lumsden

Phys. Rev. B **86**, 220509 — Published 26 December 2012

DOI: 10.1103/PhysRevB.86.220509

Effect of pressure on the neutron spin resonance in the unconventional superconductor $FeTe_{0.6}Se_{0.4}$

K. Marty,[1,*] A. D. Christianson,[1] A. M. dos Santos,[1] B. Sipos,[1] K. Matsubayashi,[2,3] Y. Uwatoko,[2,3] J. A. Fernandez-Baca,[1] C. A. Tulk,[1] T. A. Maier,[1] B. C. Sales,[1] and M. D. Lumsden[1]

[1] *Oak Ridge National Laboratory, Oak Ridge, Tennessee 37831 USA*
[2] *Institute for Solid State Physics, The University of Tokyo, Kashiwanoha, Kashiwa, Chiba 277-8581 Japan*
[3] *JST, TRiP, 5 Sanbancho, Chiyoda, Tokyo 102-0075 Japan*

(Dated: December 12, 2012)

We have carried out a pressure study of the unconventional superconductor $FeTe_{0.6}Se_{0.4}$ up to 1.5 GPa by neutron scattering, resistivity and magnetic susceptibility measurements. The neutron spin resonance energy and the superconducting transition temperature have been extracted as a function of applied pressure in samples obtained from the same crystal. Both increase with pressure up to a maximum at ≈1.3 GPa directly demonstrating a correlation between these two fundamental parameters of unconventional superconductivity. Comparison between the quantitative evolution of T_c and the resonance energy as a function of applied pressure is also discussed. These measurements serve to demonstrate the feasibility of using pressure dependent inelastic neutron scattering to explore the relationship between the resonance energy and T_c in unconventional superconductors.

PACS numbers: 74.20.Mn,74.62.Fj,74.70.Xa,78.70.Nx

Unconventional superconductors like cuprates, heavy-fermion compounds, iron pnictides and chalcogenides all share some notable features. Perhaps the most salient is the presence of static or dynamic magnetism throughout the superconducting region of the phase diagram[1,2]. A hallmark of this is a collective spin excitation that appears as a peak in the imaginary part of the dynamic susceptibility $\chi"(\mathbf{Q},\omega)$[3–12], often called the spin resonance. This resonance is localized in both wave vector and energy transfer, and appears below the superconducting transition temperature. Although still open to interpretation[14], a commonly held view is that this signal originates from a sign change of the superconducting order parameter on different parts of the Fermi surface[15]. This implies an unconventional mechanism with a repulsive interaction in momentum space, as opposed to the attractive interaction in BCS theory. Within this picture, the existence of the resonance is definitive evidence of unconventional superconductivity[16]. The observation of this signal in iron superconductors[9–13] provided further stimulus to explore the relationship between the resonance energy, ω_r, and other characteristic energy scales such as the superconducting transition temperature, T_c, or the superconducting gap, Δ[1,17–19].

Recent studies show that there is ambiguity in interpreting the relationship between T_c and ω_r[18,19], in large part due to the difficulty in separating the intrinsic and extrinsic effects of chemical doping, such as disorder, inhomogeneity, and the influence of static magnetic order. Consequently, a clean tuning parameter such as pressure has the potential to avoid these complications and yield further insight into the relationship of the resonance and unconventional superconductivity. Unfortunately, pressure dependent inelastic neutron scattering measurements are notoriously difficult and to date we are unaware of any reported studies of the spin resonance as a function of applied pressure. Thus the work presented here provides a demonstration of a new experimental approach to explore the relationship between the spin excitation spectrum and unconventional superconductivity.

The $FeTe_{1-x}Se_x$ family is a good candidate for such studies, as large single crystals can be grown and T_c shows a substantial sensitivity to applied pressure[20,21]. In particular, for compositions close to $x \approx 0.43$, the samples do not exhibit long-range magnetic order and T_c increases with pressure reaching a maximum at ≈2 GPa[22], a pressure amenable to a number of experimental techniques. Here, we present inelastic and elastic neutron scattering, resistivity and magnetic susceptibility measurements of $FeTe_{0.6}Se_{0.4}$ (T_c ≈12 K) up to 1.5 GPa. T_c and ω_r show a qualitatively similar behavior, although ω_r does not increase as much as T_c with increasing pressure, suggesting the lack of proportionality between these two energies.

The $FeTe_{0.6}Se_{0.4}$ crystal studied here was grown using a modified Bridgman technique[23]. The stoichiometry was determined by energy dispersive x-ray analysis, resulting in 1.02±0.02 for Fe, 0.6±0.02 for Te and 0.4±0.02 for Se. All the high pressure measurements were performed on samples from the same crystal growth (same large single crystal). The inelastic neutron scattering experiments under pressure were performed on the HB-3 triple axis spectrometer at the High Flux Isotope Reactor of Oak Ridge National Laboratory (ORNL) with collimations of 48'-60'-80'-120'. A McWhan piston-cylinder pressure cell[24] was used with 3M FC-75 fluorinert as the pressure medium. A 0.5 g crystal was encapsulated in the inner BeCu neutron pressure cell (⌀*h=5mm*10mm) with the $[1\bar{1}0]$ direction vertical. Room temperature neutron powder diffraction was performed using the SNAP diffractometer at the Spallation Neutron Source at ORNL. NaCl powder was ground into a 0.8 g $FeTe_{0.6}Se_{0.4}$ sample to use as a pressure calibration standard. The sample was loaded into a Paris-Edinburgh press fitted with

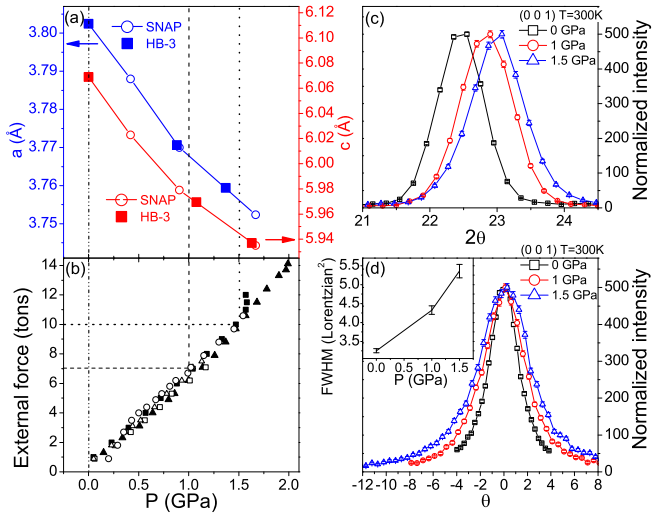

FIG. 1. (Color online) (a) Pressure dependence of the $FeTe_{0.6}Se_{0.4}$ lattice parameters a (in blue) and c (in red) measured by neutron powder diffraction on the time-of-flight diffractometer SNAP (open circles), and single crystal neutron diffraction on the triple axis spectrometer HB-3 (squares) for the single crystal used in the inelastic measurements. (b) Pressure calibration of the McWhan pressure cell as a function of the applied external force. (c) Pressure dependence of the $\theta - 2\theta$ scan on (0 0 1). (d) Evolution of the single crystal mosaic as a function of pressure. Inset: Lorentzian squared FWHM as a function of pressure.

single toroid cubic boron nitride anvils with the incident beam through the TiZr null scattering alloy gasket. Pressure was determined by application of the isothermal NaCl equation of state determined by Decker[25] to the refined lattice parameters obtained at each measured pressure from LeBail fits using the GSAS software suite[26]. High pressure resistivity measurements on a single crystal were performed in an easyLab Mcell 30. The electrical contacts were made using Dupont 4929N silver paste. The pressure was determined during the pressurization at room temperature with calibrated manganin wire and was also calculated from the applied load. Fluorinert (FC-75) was used as the pressure medium. The DC magnetization was measured on a single crystal by a commercial SQUID magnetometer (MPMS) in BeCu piston cylinder cell using Daphne7373 as the pressure medium. The pressure was calibrated using the superconducting transition of Sn.

According to the different calibration tests for the McWhan pressure cell[24] (by measuring the resistance of a manganin wire under pressure), the chosen external forces applied on the pressure cell should result in room temperature pressures of ≈0, 1 and 1.5 GPa (fig.1(b)). The lattice parameters of the large single crystal of $FeTe_{0.6}Se_{0.4}$ used for the inelastic measurements were extracted from $\theta - 2\theta$ scans through the (1 1 0) and (0 0 1) Bragg reflections (see fig.1(a) and (c)) at room temperature on the HB-3 spectrometer for the three different chosen pressure points (applied forces of respectively 1, 7 and 10 tons). The relative decrease of these lattice parameters are compared to the absolute values of these same lattice parameters obtained from neutron powder diffraction using the SNAP diffractometer. For this purpose, the first pressure point, ambient-pressure/1 ton, was considered as a common reference and the HB-3 lattice parameters were normalized to the SNAP ones. The measured relative changes (from HB-3) were then compared to the lattice parameters extracted from the SNAP data (see fig.1(a)). While the lattice parameter a shows higher values than expected from neutron powder diffraction for these pressures, the lattice parameter c shows slightly lower values, which suggests that the actual pressures at room temperature on the single crystal are close to the expected ones. One of the first visible effects of applied pressure, besides the reduction of the lattice parameters, is the broadening of the crystal mosaic. The rocking curves show a significant increase in their width (see fig.1(d) and inset). A Lorentzian-squared function provides a better description of the rocking curves than a classical Gaussian function.

In the $FeTe_{1-x}Se_x$ family, the neutron spin resonance has been shown to be two dimensional, centered at a **Q** of (1/2 1/2 L) where L indicates the irrelevant direction[11]. Above T_c, the spin excitations in $FeTe_{1-x}Se_x$ originate from an incommensurate wave vector near (1/2 1/2 L)[27]. Below T_c there is a suppression of low energy spectral weight transferred to higher energy resulting in the appearance of a resonance peak at $\omega_r \approx 6.5$ meV. Constant-Q scans at (1/2 1/2 L) were measured on the $FeTe_{0.6}Se_{0.4}$ crystal at 0, 1, and 1.5 GPa. The same, superconductivity induced redistribution of spectral weight can be seen in the constant-Q scans under applied pressure, as seen on fig.2(b) for 1 GPa and fig.2(c) for 1.5 GPa. In each case there is a clear additional signal in the inelastic spectrum corresponding to the spin resonance. While the background introduced by the pressure cell is substantial, it is not insurmountable and is indicated in fig.2(c). This definitively shows the viability of such an experiment and that the resonance can be experimentally explored as a function of applied pressure.

The resonance signal is obtained by subtracting the data collected above T_c from the data collected below T_c. This procedure results in a positive difference centered at the resonance energy ω_r and an associated negative difference at lower energy corresponding to the opening of a gap in the spin excitation spectrum. Figure 2(a) displays this signal measured on a large single crystal of the same concentration outside of the pressure cell indicating the expected resonance at ω_r=6.6 meV. For comparison, fig.2(d) shows the results of similar measurements on the 0.5 g sample (of the same concentration but different growth) within the pressure apparatus, confirming the presence of the resonance at the same energy. The effect of applied pressure on the resonance is illustrated by figures 2(e) and (f) (1 and 1.5 GPa respectively). First, ω_r is shifted to a higher energy at 1 GPa (ω_r=7.5 meV),

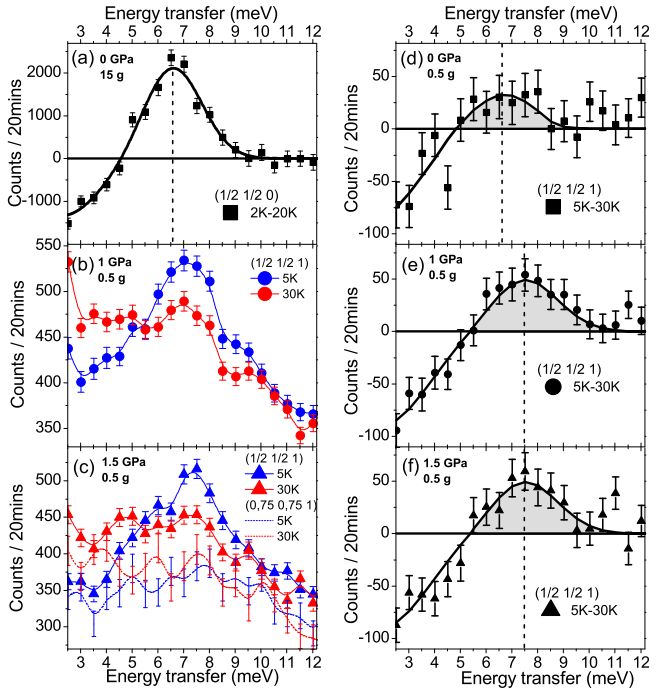

FIG. 2. (Color online) (a) Spin resonance in a 15 g single crystal of $FeTe_{0.6}Se_{0.4}$ with no applied pressure. Each point was measured for ≈7 mins. The resonance energy is indicated by a vertical dotted line. (b)-(f) All data were measured on a 0.5 g single crystal of $FeTe_{0.6}Se_{0.4}$ in the pressure cell. (b) and (c) Constant-Q scans at (1/2 1/2 1) measured below T_c (5K, blue) and above T_c (30K, red) at respectively 1 GPa (circles, 80mins/point) and 1.5 GPa (triangles, 60 mins/point). At 1.5 GPa, background constant-Q scans (dotted lines) measured at (0.75 0.75 1) for 20 mins/point are shown for T=5 K (blue) and T=30 K (red). (d) Spin resonance at 0 GPa. Each point was measured for 40 mins. The resonance energy, the same as (a), is indicated by a vertical dotted line. (e) Same as (d) for 1 GPa and 80 mins/point. (f) Same as (d) and (e) for 1.5 GPa and 60 mins/point. The line and shaded area are the same as 1 GPa to emphasize the similar spectral weight and resonance energy for both pressures. Solid lines are guide for the eye. All data were normalized to 20 mins/point.

but does not increase further at higher pressure. Second, the spectral weight enhancement below T_c follows the same qualitative behavior as ω_r with a clear increase at 1 GPa and does not increase further at 1.5 GPa.

The large thermal mass of the pressure cell combined with long counting times prohibited an accurate determination of T_c from the onset of the resonance. Therefore the pressure dependence of T_c was determined from resistivity and magnetic susceptibility measurements on single crystal samples from the same growth as the crystal used for the inelastic neutron scattering measurements (see fig.3). Although different methods are commonly used to extract T_c from resistivity data, for completeness we adopt two metrics: (1) the onset of the drop in resistivity due to the appearance of superconductivity (T_c onset) and (2) the temperature at which the resistivity achieves the minimum value (T_c min).

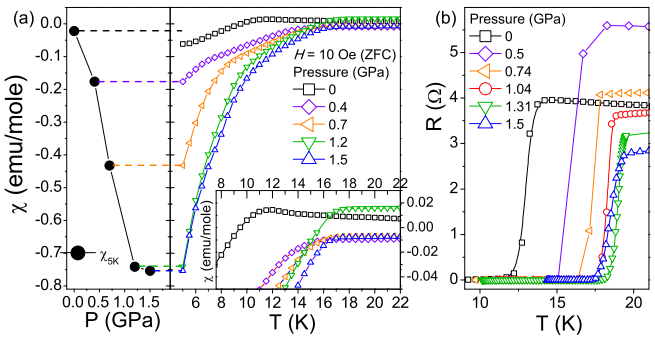

FIG. 3. (Color online) (a) Temperature dependence of magnetic susceptibility χ_{mag} for various applied pressure in the 0-1.5 GPa range. Inset: zoom on χ_{mag}(T) in the superconducting transition zone. Left panel: Lowest value of χ_{mag}, proportional to the screening effect in the sample. (b) Temperature dependence of electrical resistivity for various applied pressure in the 0-1.5 GPa range.

The magnetic susceptibility data show broad transitions (see fig.3(a)), as previously observed for lower concentrations of Se ($x \leq 0.4$). In those cases, T_c is usually defined as the temperature where χ_{mag} starts to decrease[28]. Although the broadness of the transition potentially indicates a distribution of T_cs, the energy of the resonance from the neutron scattering data is well defined, suggesting a unique bulk behavior[29]. For the following discussion, we will use the definition $T_c(\chi_{mag})$ as described above. Although we believe our neutron scattering data is consistent with a narrow distribution of transition temperatures, we note that a hypothetical distribution of T_cs in our sample together with a sharp resonance signal can only be understood if the resonance energy and T_c are effectively decoupled[29].

Here, as shown in fig.4(a), despite a constant offset in absolute value, T_c obtained from all three methods show similar qualitative behavior, supporting the reliability of our definitions. At ambient pressure, previous measurements for this concentration suggest a T_c of about 14 K as extracted from the onset of resistivity. Our value of 13.6±0.4 K is slightly less than this value. Such discrepancies are not uncommon, this is precisely why we use pressure to overcome this problem by measuring the relative change of T_c in one sample rather than absolute values. Here, T_c increases with pressure by ≈ 50% at ≈ 1.3 GPa, then remains constant or decreases slightly at higher pressures. Consistently, similar qualitative behavior was observed in other members of the $FeTe_{1-x}Se_x$ family[20–22].

The lowest value of χ_{mag}, at the lowest temperature (5 K), is a manifestation of the screening effect in the sample. χ_{5K} strongly decreases with applied pressure, reaching a plateau above ≈1 GPa (see fig.3(a) left). This increased screening effect could indicate an enhancement of the superconducting volume fraction with pressure. As

the strength of the resonance signal scales with superconducting volume fraction, we would expect a change in volume fraction would result in a change in inelastic neutron scattering intensity, as observed experimentally (see figs.2(d)-(f)). Whether the intensity increase is due to a changing volume fraction or is caused by a direct link between T_c and the resonance spectral weight remains unclear.

To provide further insight into the implications of our measurements we make the assumption that the T_cs which have been determined from bulk measurements are representative of the behavior of the large single crystal. Under this assumption ω_r(P) and T_c(P) can be relevantly compared. Figure 4(a) displays such a comparison, where ω_r is expressed in units of Kelvin and scaled by a constant to coincide with the lowest estimate of T_c(P) at ambient pressure. Despite a qualitative similarity in the behavior of ω_r(P) and T_c(P), the resonance energy does not increase nearly as rapidly as T_c. To further clarify this point, fig.4(b) shows the ratio ω_r/k_BT_c as a function of T_c. Both figs.4(a) and (b) suggest that ω_r is not proportional to T_c. This fact is independent of the definition we choose for T_c. These measurements show the feasibility of inelastic neutron scattering as a function of applied pressure for such studies and future measurements will be of high interest to compare these results with other unconventional superconductors.

A comparison of this observation to the data obtained from multiple 122 materials[19] is particularly interesting. Contrary to the $FeTe_{1-x}Se_x$ family, these materials have a q_z dependent resonance mode where the ratio, ω_r/k_BT_c, is constant for $q_z=\pi$ and seems to vary with T_c for $q_z=0$. Interestingly, the data presented in fig.4(b) is qualitatively similar to the $q_z=0$ data for the 122 compounds. This suggests that when 3-dimensional, the resonance relevant for superconductivity, and which should be compared to either T_c or Δ, might be the one measured at $q_z=0$.

It is worth noting that for the 122 materials, the highest ratios ω_r/k_BT_c (at $q_z=0$) are obtained for the lowest concentrations of dopant, where electronic correlations are stronger. This is consistent with our observations of ω_r/k_BT_c decreasing with applied pressure in $FeTe_{0.6}Se_{0.4}$, as applying pressure likely increases orbital overlap and hybridization, implying a more itinerant and less correlated system. Within this context, the ratio of these energy scales relevant in unconventional superconductivity, ω_r/k_BT_c, seems to be an indication of the strength of the correlations in the system. This is also supported by higher observed ratios of ω_r/k_BT_c in cuprates, which are notoriously more correlated[18].

Since the neutron spin resonance is often compared to the superconducting gap Δ[1,18,19], it is interesting to examine the consequences of our results for the underlying pairing mechanism. Unfortunately, no data of Δ as a function of pressure are available. Therefore we discuss our results in the context of a simple Hubbard model and consider the aforementioned model of sign change of the

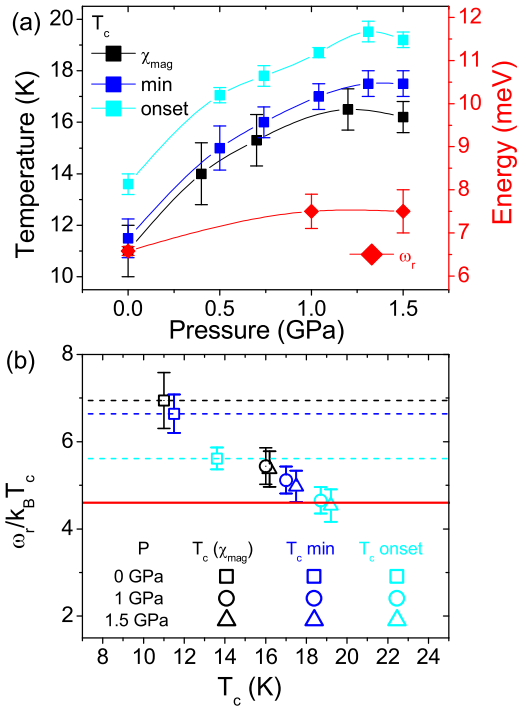

FIG. 4. (Color online) (a) Pressure dependence of ω_r (in red) and T_c as defined by the magnetic susceptibility (in black), and the resistivity (T_c min in dark blue, T_c onset in light blue). (b) T_c dependence of the ω_r/k_BT_c ratio of $FeTe_{0.6}Se_{0.4}$ for all pressures (squares for 0 GPa, circles for 1 GPa and triangles for 1.5 GPa), and all definitions of the transition temperature. The horizontal dotted lines correspond to the value of ω_r/k_BT_c at 0 GPa for all three definitions of T_c. The horizontal red line corresponds to ω_r/k_BT_c=4.6 as previously observed for iron superconductors[17,18].

superconducting order parameter[15]. Within this context, a screened, on-site, intra-orbital Coulomb interaction, U, renormalizes ω_r to a value lower than the energy of the particle-hole continuum, 2Δ[30,31]. Pressure increases orbital overlap, effectively reducing U, and in turn increasing the ratio of $\omega_r/2\Delta$. In the very weak-coupling limit, we expect $\omega_r/2\Delta \approx 1$[30,31]. For either increasing or constant $\omega_r/2\Delta$, the observed decrease of ω_r/k_BT_c between 0 and 1 GPa implies a reduction of the superconducting pairing strength $2\Delta/k_BT_c$ (even though paradoxically the energy scale T_c has risen).

To conclude, this work further demonstrates that inelastic neutron scattering in conjunction with applied pressure is a powerful approach to unraveling the relationship between spin excitations and unconventional superconductivity. We have performed a pressure dependent study of the neutron spin resonance and superconducting transition temperature of an unconventional $FeTe_{0.6}Se_{0.4}$ superconductor up to 1.5 GPa. Free from any constraint induced by chemical substitution, we have shown that the energy and the intensity of the resonance increase with applied pressure up to 1 GPa then stabilize. The similarity of this qualitative pressure dependent

behavior with that of T_c confirms a correlation between those two characteristic energies and the important role of spin excitations in Fe-based unconventional superconductivity.

ACKNOWLEDGMENTS

Research at ORNL is sponsored by the Scientific User Facilities Division and the Materials Sciences and Engineering Division, Office of Basic Energy Sciences, U.S. DOE. Work in Japan was supported by a Grant-in-Aid for Research (Nos. 21340092, 20102007, and 19GS0205) from the Ministry of Education, Culture, Sports, Science, and Technology, Japan. We acknowledge discussions with D. J. Singh and D. Mandrus. We thank E. D. Specht for the use of the X-ray Laüe and S. Kulan and J. J. Molaison for technical support.

* Present address: SPINTEC, UMR-8191, CEA/CNRS/UJF/GINP, INAC, F-38054 Grenoble, France

[1] S. Hüfner *et al.*, Rep. Prog. Phys. **71**, 062501 (2008)
[2] M. D. Lumsden and A. D. Christianson, J. Phys.: Condens. Matter **22**, 203203 (2010)
[3] J. Rossat-Mignod *et al.*, Physica C **185**, 8692 (1991)
[4] H. F. Fong, *et al.*, Nature **398**, 588591 (1999)
[5] P. Dai, *et al.*, Nature **406**, 965968 (2000)
[6] H. He, *et al.*, Science **295**, 10451047 (2002)
[7] N. K. Sato *et al.*, Nature **410**, 340343 (2001)
[8] C. Stock, C. Broholm, J. Hudis, H. J. Kang and C. Petrovic, Phys. Rev. Lett. **100**, 087001 (2008)
[9] A. D. Christianson, *et al.*, Nature **456**, 930 (2008)
[10] M. D. Lumsden *et al.*, Phys. Rev. Lett. **102**, 107005 (2009)
[11] Y. M. Qiu *et al.*, Phys. Rev. Lett. **103**, 067008 (2009)
[12] J. T. Park *et al.*, Phys. Rev. Lett. **107**, 177005 (2011)
[13] P. Babkevich *et al.*, Phys. Rev. B **83**, 180506(R) (2011)
[14] H. Kontani and S. Onari, Phys. Rev. Lett. **104**, 157001 (2010)
[15] N. Bulut and D. J. Scalapino, Phys. Rev. B **53**, 5149 (1996)
[16] M. Eschrig, Adv. Phys. **55**, 47 (2006)
[17] J. Paglione and R. L. Greene, Nature Phys. **6**, 645-658 (2010)
[18] G. Yu *et al.*, Nature Phys. **5**, 873 (2009)
[19] D. S. Inosov *et al.*, Phys. Rev. B **83**, 214520 (2011)
[20] Y. Mizuguchi *et al.*, Appl. Phys. Lett **93**, 152505 (2008)
[21] K. Horigane *et al.*, J. Phys. Soc. Jpn. **78**, 063705 (2009)
[22] N. C. Gresty *et al.*, J. Am. Chem. Soc. **131**(46), 16944 (2009)
[23] B. C. Sales *et al.*, Phys. Rev. B **79**, 094521 (2009)
[24] A. Onodera *et al.*, Jpn. J. Appl. Phys. **26**, 152 (1987)
[25] D. L. Decker, J. Appl. Phys., **42**, 3239-3244 (1971)
[26] A. C. Larson and R.B. Von Dreele, "General Structure Analysis System (GSAS)", Los Alamos National Laboratory Report LAUR **86**, 748 (2000)
[27] M. D. Lumsden *et al.*, Nature Phys. **6**, 182 (2010)
[28] T. J. Liu *et al.*, Nature Mat. **9**, 716 (2010)
[29] See Supplementary information at [URL will be inserted by publisher] for a discussion about the sample quality.
[30] I. I. Mazin and V. M. Yakovenko, Phys. Rev. Lett. **75**, 4134 (1995)
[31] D. Manske, I. Eremin and K. H. Bennemann, Phys. Rev. B **63**, 054517 (2001)